# Complex magnetic order and spin chirality on the Kagomé lattices of $BaMn_{2.49}Ru_{3.51}O_{11}$ and $BaFe_{3.26}Ti_{2.74}O_{11}$

L. Shlyk,[1,a] S. Parkin,[2] and L. E. De Long[1]
[1]*Department of Physics and Astronomy, University of Kentucky, Lexington, Kentucky 40506-0055, USA*
[2]*Department of Chemistry, University of Kentucky, Lexington, Kentucky 40506-0055, USA*

(Presented 21 January 2010; received 30 October 2009; accepted 15 January 2010; published online 21 April 2010)

Anomalies in the magnetization of single-crystal $BaMn_{2.49}Ru_{3.51}O_{11}$ at temperatures $T_1=183$ K, $T_2=171$ K, and $T_3=128$ K, signal complex magnetic order induced by competing ferro- and antiferromagnetic correlations and magnetic frustration within the Kagomé (hexagonal ab-) plane. The $T_2$- and $T_3$-anomalies and unconventional transverse magnetoresistance are observed only for applied field $H$ directed in the Kagomé plane, suggesting a topological Hall effect is generated by nonzero scalar chirality of spins canted out of the Kagomé plane, but is suppressed in a collinear structure induced by only modest $H \perp c$. In contrast, the magnetic susceptibility of an isostructural $BaFe_{3.26}Ti_{2.74}O_{11}$ single-crystal reveals magnetic transitions at $T_1=250$ K and $T_2=85$ K for $H$ oriented both parallel and perpendicular to the c-axis. The rapid low-field increase of the magnetic moment at $\mu_o H<1$ T, followed by nonsaturation with a near-linear increase at high fields, are typical of a canted antiferromagnet or ferrimagnet. © *2010 American Institute of Physics*. [doi:10.1063/1.3364060]

Frustration of antiferromagnetic (AFM) interactions by crystallographic symmetry is of current interest, and is marked by highly degenerate, noncollinear magnetic ground states that break chiral symmetry. A representative frustrated system is a Kagomé lattice formed from corner-sharing triangles. The R-type ferrites $BaM_2Ru_4O_{11}$ (M=Fe, Mn, and Co) crystallize in the hexagonal $P6_3/mmc$ structure[2,3] in which layers of edge-sharing octahedra $M(2)O_6$ form a Kagomé sublattice within the a-b plane. The Kagomé planes are connected along the c-axis by face-sharing $M(1)O_6$ octahedra and trigonal bipyramids $M(3)O_5$ (Fig. 1).

$(Ba,Sr)M_{2\pm x}Ru_{4\mp x}O_{11}$ (M=Fe or Co) exhibit electric and magnetic properties that can be widely varied by simple chemical substitution of 3d-elements, or by varying the relative concentration of 3d-elements and 4d-Ru over a wide homogeneity range.[4,5] In spite of potential magnetic frustration on the Kagomé sublattice, some of these compositions exhibit a unique coexistence of narrow-gap semiconductivity with ferrimagnetic order at unusually high critical temperatures $T_C \sim 480$ K. These properties, together with a large anomalous Hall effect, make R-type ferrites attractive for spintronic applications.

We have found R-type ferrites of composition $BaM_{2\pm x}T_{4\mp x}O_{11}$ (M=Fe and Mn; T=Ru and Ti) exist over a homogeneity range generated by variable occupation of the octahedral M(1) and M(2) sites by 3d (Fe, Ti, and Mn) and 4d (Ru) elements, whereas the trigonal-pyramidal M(3) sites are exclusively occupied by 3d (Fe or Mn) elements.[5] Here we focus on $BaMn_{2.49}Ru_{3.51}O_{11}$ and $BaFe_{3.26}Ti_{2.74}O_{11}$ single crystals that undergo several successive magnetic transitions.

Single crystals with maximum basal-plane width 1.5 mm and thickness around 0.05 mm were grown from a $BaCl_2$ flux, as described elsewhere.[4] Sample compositions were determined from x-ray refinements and microprobe analysis. X-ray diffraction data were collected at $T=90.0(2)$ K on a Nonius Kappa CCD Diffractometer using Mo K$\alpha$ radiation. The final full-matrix, least-squares refinement converged to $R_1=0.0375\%$, $wR_2=0.1040\%$ [with refined lattice parameters a=5.8370(8) Å, c=13.616(3) Å] for $BaFe_{3.26}Ti_{2.74}O_{11}$, and to $R_1=0.0143\%$, $wR_2=0.0369\%$ [with refined lattice parameters a=5.8754(8) Å, c=13.515(3) Å] for $BaMn_{2.49}Ru_{3.51}O_{11}$. The dc magnetic moment of oriented single crystals was measured over a temperature range $5\ \text{K} \le T \le 300$ K in applied magnetic fields $0 \le \mu_o H \le 5$ T using a Quantum Design MPMS5 Magnetometer. Longitudinal and transverse magnetoresistivities, $\rho_{xx}(T)$ and $\rho_{xy}(H,T)$, respec-

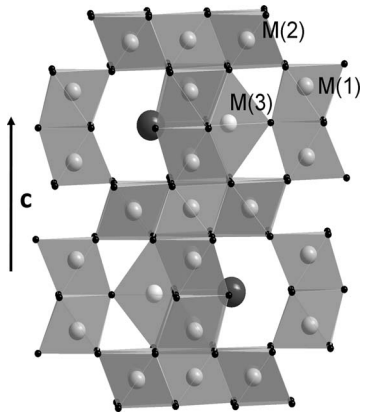


FIG. 1. Crystal structure of R-type ferrites. The M(1) (4e) sites are predominantly occupied by Ru, the M(2) (6g) sites on the Kagomé sublattice are occupied by Ru and appropriate 3d-elements, and the M(3) (2d) sites are predominantly occupied by the appropriate 3d-elements (Refs. 4 and 5).

[a]Author to whom correspondence should be addressed. Tel.: 859 218 6526. Electronic mail: lshlyk@gmail.com.

 

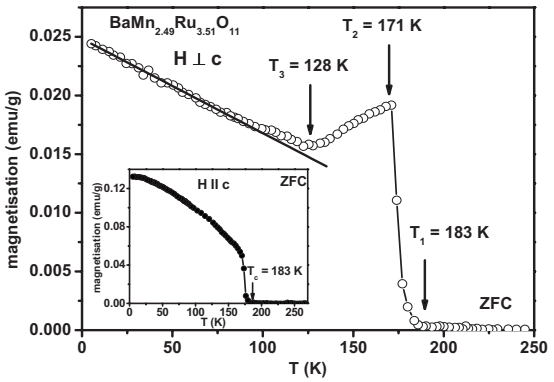


FIG. 2. Temperature dependence of the ZFC magnetization $M_{\perp}(T,H)$ of single-crystal $BaMn_{2.49}Ru_{3.51}O_{11}$. Arrows designate magnetic transition temperatures. The solid line illustrates the linear dependence below $T_3 = 128$ K. The lower inset: ZFC magnetization $M_{\parallel}(T)$ vs temperature of single-crystal $BaMn_{2.49}Ru_{3.51}O_{11}$. ZFC mode is determined as a mode with a small residual field of only a few oersteds after complete degaussing of the superconducting quantum interference device.

tively, were measured using the MPMS5 external device control option and a dc four-probe method with currents $5\ \text{mA} \leq J \leq 20\ \text{mA}$ directed in the a-b plane.

ZFC data for the magnetization $M_{\parallel}(T)$ of $BaMn_{2.49}Ru_{3.51}O_{11}$ measured for $H \parallel$ c-axis (Fig. 2, inset) reveal a spontaneous magnetization that reflects ferromagnetic (FM) correlations below $T_C = 183$ K, consistent with previous polycrystalline data[3] (zero-field-cooled (ZFC) and field-cooled (FC) $M(T,H)$ curves are identical in their shape, indicating magnetic domain formation does not complicate these data). The magnetization curves for $H \parallel$ c are characteristic of a soft FM material with a coercive field $H_{c\parallel} = 400$ Oe at $T = 5$ K (Fig. 3, upper inset). Distinct magnetic anisotropy (see Figs. 2 and 3) indicates the c-axis is the easy direction.

The ZFC magnetization $M_{\perp}(T,H)$ exhibits three striking anomalies for $H \perp$ c: an abrupt increase just below $T_1 = 183$ K, a cusp at $T_2 = 171$ K, and a sharp minimum at $T_3 = 128$ K that marks a strong, linear increase of $M_{\perp}(T,H)$ with decreasing $T < T_3$, as shown in Fig. 2. The sharp decrease of $M_{\perp}(T,H)$ below $T_2 = 171$ K indicates dominant

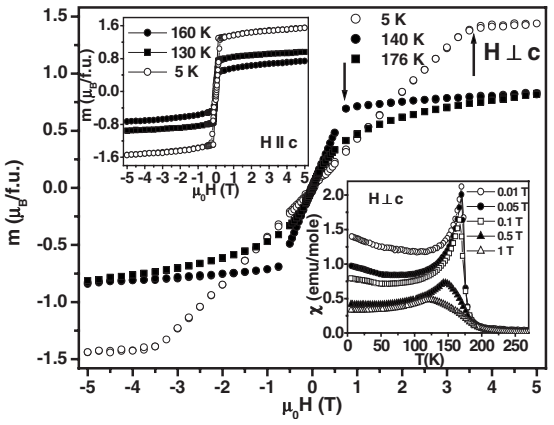


FIG. 3. Magnetic moment $m_{\perp}$ vs applied field $H \perp$ c for several temperatures $T$ for single-crystal $BaMn_{2.49}Ru_{3.51}O_{11}$. The lower inset shows $\chi_{\perp}(T,H)$ at different applied fields $\mu_o H \perp$ c. The upper inset shows $m_{\parallel}(T,H)$ vs applied field $\mu_o H \parallel$ c for several temperatures.

AFM interactions, whereas the linear increase of $M_{\perp}(T,H)$ below $T_3 = 128$ K reflects residual FM correlations. The lower inset in Fig. 3 shows the susceptibility $\chi_{\perp}(T,H)$ in fields $0.01\ \text{T} \leq \mu_o H \leq 1\ \text{T}$, which slowly broaden and shift the $T_2$-anomaly to lower temperatures, but rapidly make the $T_3$-anomaly indistinct.

The field dependences of the magnetic moment $m_{\perp}(T,H)$ shown in Fig. 3 reflect two distinct regions for $T < 167$ K: a slow, linear increase of $m_{\perp}$ ends at a critical field $H^*(T)$ (whose magnitude increases with decreasing $T$) at which $dm_{\perp}/dH$ is discontinuous, and is followed by a saturated regime above $H^*(T)$. This behavior resembles that of simple AFM materials, where $m(H)$ barely changes in the low-field collinear phase, then abruptly jumps into a canted structure at a spin flop transition followed by a strong linear increase of $m(H)$ ending abruptly at FM saturation. (Here, an applied $H \perp$ c acts in conjunction with the exchange field along the easy c-axis to create the spin flop for the spins frustrated within the a-b planes). The strong linear increase and absence of any jump in $m_{\perp}(H)$ in Fig. 3 suggests a canted spin arrangement (dominated by AFM correlations) is present below $T_2 = 171$ K. The low-field, linear $m_{\perp}(H)$ is replaced by nonlinear FM behavior above 171 K, confirming FM correlations dominate AFM correlations for $T > T_2$.

The above observations signal complex magnetic order, consistent with previous powder neutron diffraction data[2] for *polycrystalline* $BaMn_2Ru_4O_{11}$: the M(1) sites were judged nonmagnetic, the M(3) sites ordered ferromagnetically parallel to the c-axis, and the M(2) sites ordered in a compensated triangular motif, characteristic of a frustrated lattice with AFM nearest-neighbor interactions. At $T = 100$ K, the data were refined with an *in-plane*, "q=0" structure having uniform *vector chirality* $\boldsymbol{K_V} = [2/(3\sqrt{3})](\boldsymbol{S}_1 \text{x} \boldsymbol{S}_2 + \boldsymbol{S}_2 \text{x} \boldsymbol{S}_3 + \boldsymbol{S}_3 \text{x} \boldsymbol{S}_1)$ (where $S_i$ [i=1–3] are spins located at the vertices of a Kagomé triangular plaquette). Below 100 K, the M(2) spins cant out of the a-b plane, inducing nonzero *scalar chirality* $K_S \equiv \mathbf{S}_1 \cdot (\mathbf{S}_2 \times \mathbf{S}_3)$, and a continuous increase of magnetic peak intensity that culminates in an ordered moment $m = 3.3\ \mu_B$ at $T = 3.6$ K.

The spin canting out of the Kagomé plane can generate a topological Hall effect (THE) driven by nonzero $K_S$.[1] The Hall resistivity of ferromagnets is usually expressed as

$$\rho_{xy} = R_o H + 4\pi M R_s, \tag{1}$$

where $R_o$ is the "normal" Hall coefficient resulting from the Lorentz force and $R_s$ is the "anomalous" Hall coefficient that is dependent upon the magnetization $M$ and spin-orbit coupling.[6,7] The low-field Hall effect of FM materials is dominated by the anomalous term (AHE) identified by a field dependence that follows $M(T,H)$ below $T_C$.[6] We measured $\rho_{xy}(H,T)$ for $BaMn_{2.49}Ru_{3.51}O_{11}$ with in-plane current $\boldsymbol{J} \perp H \parallel$ c (easy direction), which should induce a collinear state that suppresses spin chirality and the THE. As expected, $\rho_{xy}$ exhibits a nonlinear field dependence only for $H \ll 1.0$ T where the AHE dominates (upper inset, Fig. 4). Above 1.0 T, both $m_{\parallel}(H)$ (upper inset, Fig. 3) and $\rho_{xy}$ exhibit a weakly linear normal behavior.

In order to minimize the normal Hall term due to the Lorentz force, we employed an unconventional configuration

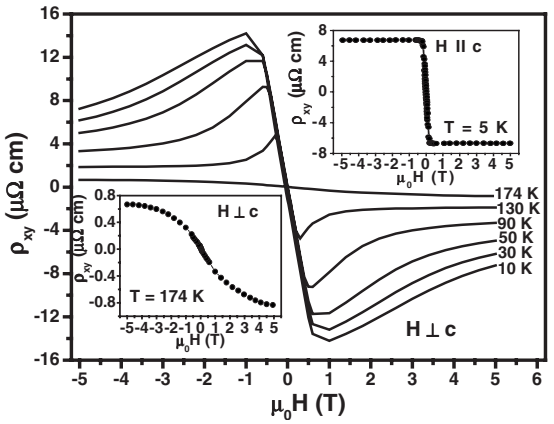


FIG. 4. Transverse resistivity $\rho_{xy}$ vs magnetic field $H \perp c$ for single-crystal $BaMn_{2.49}Ru_{3.51}O_{11}$ at different temperatures. The upper inset shows $\rho_{xy}$ vs magnetic field $H \| c$ (easy axis) at temperature $T=5$ K. The lower inset shows $\rho_{xy}$ for a $BaMn_{2.49}Ru_{3.51}O_{11}$ single-crystal at $T=174$ K and $H \perp c$.

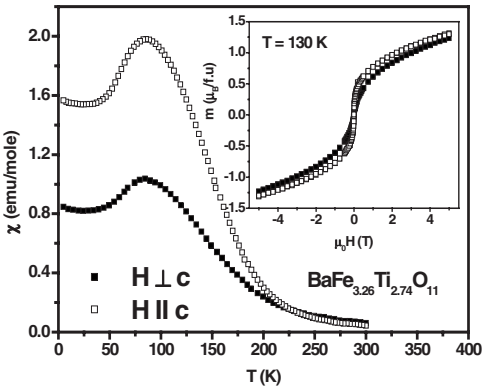


FIG. 5. Temperature dependence of the FC dc magnetic susceptibility $\chi(T)$ of single-crystal $BaFe_{3.26}Ti_{2.74}O_{11}$ for $H \perp c$ and $H \| c$ at applied magnetic field $\mu_o H=0.1$ T. Inset shows the magnetic moment $m$ vs $\mu_o H$ at temperature $T=130$ K.

with $\boldsymbol{J} \| H \perp c$, where $\rho_{xy}(T,H)$ should depend only on the AHE of the c-axis magnetization on the M(2) and M(3) sites, and the THE contribution of the nonzero $K_S$ of the M(2) sublattice. In this geometry, $\rho_{xy}(T,H)$ does not follow the saturation behavior of $m(H)$ for $T<T_2=171$ K (compare Figs. 3 and 4), but exhibits a strong decrease with increasing field for $|H|>H^*$, which marks a sharp change in $d\rho_{xy}(H)/dH$ (Fig. 4).

The unusual nonmonotonic field dependence of $\rho_{xy}$ can be explained in terms of field suppression of $K_S$. At low fields the intermediate canting angle of noncollinear M(2) spins induces a relatively large $K_S$ and resulting THE; further increases of field align the M(2) spins along $H$, which reduces $K_S$ and $\rho_{xy}$. $BaMn_{2.49}Ru_{3.51}O_{11}$ is remarkable in that the peak in $\rho_{xy}$ approximately *triples in magnitude* between $T=130$ and 10 K in fields well below 1 T (Fig. 4). Moreover, for $T>171$ K, $\rho_{xy}$ displays a monotonic field dependence typical of ferromagnets (lower inset, Fig. 4), implying there is *no* $K_S$ to drive a THE for $T_2<T<T_1$.

Magnetic susceptibility measurements on a $BaFe_{3.26}Ti_{2.74}O_{11}$ single-crystal reveal two magnetic transitions for applied field $H$ oriented both parallel and perpendicular to the c-axis: A slow increase of $\chi(T)$ below $T_1=250$ K is followed by a maximum at $T_2=85$ K, with a distinct magnetic anisotropy that indicates the c-axis is the easy direction, as shown in Fig. 5. The rapid increase of $m(H)$ in low fields and near-linear variation without saturation at $\mu_o H>1.2$ T (both above and below 85 K) are typical of a canted antiferromagnet or ferrimagnet.[10] Coercive fields $\mu_o H_{c\perp}=1.0$ T and $\mu_o H_{c\|}=0.75$ T perpendicular and parallel to the c-axis, respectively, are observed at $T=5$ K; this anisotropy is greatly reduced ($\mu_o H_{c\perp}=\mu_o H_{c\|}=4.5\times10^{-4}$ T) at $T=130$ K (inset, Fig. 5). Above 250 K, the susceptibility $\chi(T)$ is isotropic, and $m(H)$ varies linearly with magnetic field. A Curie–Weiss fit of $\chi(T)$ in the temperature interval $260\ K<T<360$ K yields an effective magnetic moment $\mu_{eff}=4.73\ \mu_B$ and a positive Weiss temperature $\theta_P=220$ K that indicates dominant FM interactions. The basal-plane electrical resistance of $BaFe_{3.26}Ti_{2.74}O_{11}$ is $R_{300}\sim20$ MΩ, which demonstrates the complete replacement of Ru (4d-electrons) with more localized Ti (3d-electrons) results in a strongly gapped insulator.

In summary, single crystals of $BaMn_{2.49}Ru_{3.51}O_{11}$ and $BaFe_{3.26}Ti_{2.74}O_{11}$ exhibit complex magnetic order driven by competing interactions on a frustrated lattice with a noncentrosymmetric structure. The striking behavior of $BaMn_{2.49}Ru_{3.51}O_{11}$ reflects frustrated two-dimensional spin correlations for $171\ K<T<183$ K, which favor an in-plane, "q=0" structure with zero $K_S$ on the Kagomé sublattice, consistent with neutron diffraction data[3] for polycrystalline $BaMn_2Ru_4O_{11}$. A c-axis moment grows below $T_2=171$ K, caused by Dzyaloshinsky–Moriya interactions[8,9] appropriate for spins in a noncentrosymmetric structure with nonzero $K_S$. The slow saturation of $m(T,H)$ with decreasing $T$, or increasing $H \perp c$, indicates an evolution from canted spins with AFM correlations within the Kagomé plane, to a collinear FM arrangement. The unusually large, nonmonotonic field dependence of $\rho_{xy}$ observed in single-crystal $BaMn_{2.49}Ru_{3.51}O_{11}$ for $\boldsymbol{J} \| H \perp c$ also results from the field-dependent canting of the M(2) spins out of the Kagomé plane, which creates a large THE driven by nonzero scalar spin chirality that can be controlled and suppressed by only modest applied fields $<1$ T.

## ACKNOWLEDGEMENT

Research at the University of Kentucky was supported by U.S. DOE Grant No. DOE-FGØ2-97ER45653.

[1] Y. Taguchi, Y. Oohara, H. Yoshizawa, N. Nagaosa, and Y. Tokura, Science **291**, 2573 (2001).
[2] M. C. Cadee and D. J. W. Ijdo, J. Solid State Chem. **52**, 302 (1984).
[3] M. L. Foo, Q. Huang, J. W. Lynn, W.-L. Lee, T. Klimczuk, I. S. Hagemann, N. P. Ong, and R. J. Cava, J. Solid State Chem. **179**, 563 (2006).
[4] B. Schüpp-Niewa, L. Shlyk, S. Kryukov, L. E. De Long, and R. Niewa, Z. Naturforsch. B **62**, 753 (2007).
[5] L. Shlyk, S. Kryukov, B. Schüpp-Niewa, R. Niewa, and L. E. De Long, Adv. Mater. **20**, 1315 (2008).
[6] R. Karplus and J. M. Luttinger, Phys. Rev. **95**, 1154 (1954).
[7] L. Berger, Phys. Rev. B **2**, 4559 (1970).
[8] I. Dzyaloshinsky, J. Phys. Chem. Solids **4**, 241 (1958).
[9] T. Moriya, Phys. Rev. **120**, 91 (1960).
[10] R. L. Carlin, *Magnetochemistry* (Springer-Verlag, Berlin, 1986).